



D_{3h} [A-CE₃-A]⁻ (E = Al and Ga, A = Si, Ge, Sn, and Pb): A new class of hexatomic mono-anionic species with trigonal bipyramidal carbon

Yan-Bo Wu,^{1,a)} Yan-Qin Li,¹ Hui Bai,¹ Hai-Gang Lu,¹ Si-Dian Li,¹ Hua-Jin Zhai,¹ and Zhi-Xiang Wang^{2,a)}

¹Institute of Molecular Science, Key Laboratory of Chemical Biology and Molecular Engineering of Education Ministry, Shanxi University, Wucheng Road 92#, Taiyuan 030006, People's Republic of China

²College of Chemistry and Chemical Engineering, University of Chinese Academy of Sciences, Yuquan Road 19#, Beijing 100049, People's Republic of China

(Received 16 September 2013; accepted 20 February 2014; published online 11 March 2014)

The non-classical trigonal bipyramidal carbon (TBPC) arrangement generally exists as transition states (TSs) in nucleophilic bimolecular substitution (S_N2) reactions. Nevertheless, chemists have been curious about whether such a carbon bonding could be stable in equilibrium structures for decades. As the TBPC arrangement was normally realized as cationic species theoretically and experimentally, only one anionic example ([At-C(CN)₃-At]⁻) was computationally devised. Herein, we report the design of a new class of anionic TBPC species by using the strategy similar to that for stabilizing the non-classical planar hypercoordinate carbon. When electron deficient Al and Ga were used as the equatorial ligands, eight D_{3h} [A-CE₃-A]⁻ (E = Al and Ga, A = Si, Ge, Sn, and Pb) TBPC structures were found to be the energy minima rather than TSs at both the B3LYP and MP2 levels. Remarkably, the energetic results at the CCSD(T) optimization level further identify [Ge-CAl₃-Ge]⁻ and [Sn-CGa₃-Sn]⁻ even to be the global minima and [Si-CAl₃-Si]⁻ and [Ge-CGa₃-Ge]⁻ to be the local minima, only slightly higher than their global minima. The electronic structure analyses reveal that the substantial ionic C-E bonding, the peripheral E-A covalent bonding, and the axial mc-2e (multi center-two electrons) bonding play roles in stabilizing these TBPC structures. The structural simplicity and the high thermodynamic stability suggest that some of these species may be generated and captured in the gas phase. Furthermore, as mono-anionic species, their first vertical detachment energies are differentiable from those of their nearest isomers, which would facilitate their characterization via experiments such as the negative ion photoelectron spectroscopy. © 2014 AIP Publishing LLC. [<http://dx.doi.org/10.1063/1.4867364>]

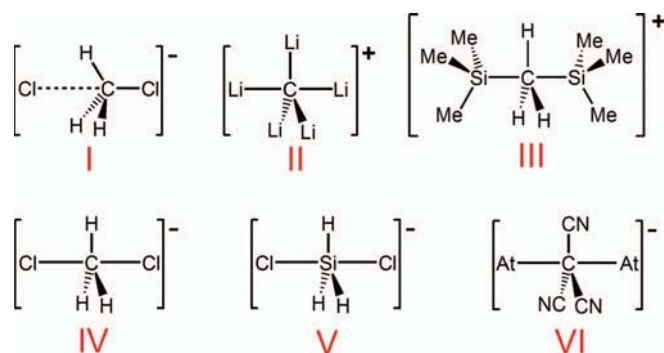
I. INTRODUCTION

Carbon predominately adopts the classical linear *sp*, planar trigonal *sp*², and tetrahedral *sp*³ hybridization bonding to bond to its neighbors. Besides, compounds featuring the non-classical carbon bonding pattern have also been well characterized. Sparked by the curiosity whether a transition state (TS) structure with a planar tetracoordinate carbon (ptC) can be stabilized, strategies to achieve the stable planar hypercoordinate carbon (phC) arrangement have been developed.¹⁻⁸ Meanwhile, the trigonal bipyramidal carbon (TBPC) arrangement has also attracted attention for more than three decades. The quest for the TBPC arrangement originated from the curiosity whether the arrangement featuring a central pentacoordinate carbon at the midpoint of the Walden inversion process of S_N2 reactions could be a metastable intermediate.⁹⁻¹¹ Due to the rigidity of *sp*³ tetrahedral carbon, the TBPC structures are normally the transition states and will be converted into the equilibrium structures featuring a long axial bond, a localized axial bond, and a pyramidal middle unit, as exemplified by [Cl-CH₃-Cl]⁻ (see I in Scheme 1).

However, the TBPC arrangement has been found in the equilibrium structures of several cationic species. Examples include D_{3h} CH₃A₂⁺ (A = Li, Na, BeH, and MgH), D_{3h} CLi₅⁺ (Scheme 1-II), Si₂(CH₃)₇⁺ (Scheme 1-III), and CH₃(XH_{*n*})₂⁺ (X = group 1, 2, 13, and 14 elements),¹²⁻¹⁶ among which CH₃Li₂⁺, CLi₅⁺, and Si₂(CH₃)₇⁺ were confirmed experimentally.^{13,14,16} As these cationic TBPC species were scaffold-free, TBPC could also be harnessed by molecular scaffolds such as anthracene^{10,11} and 2,6-bis(*p*-substituted phenyloxymethyl) benzene.¹⁷ It should be pointed out that the X-ray structure of these “scaffold-confined” TBPC species have the interatomic distances between the central carbon and the axial atoms (A) significantly longer than the normal C-A bond lengths.

In 2005, using anthracene as a scaffold was attempted to achieve anionic TBPC species, but was not successful, as revealed by its X-ray structure which indicated a classical *sp*³ carbon with a short axial C-O distance (1.470 Å) and a very long axial C-O distance (2.991 Å).¹⁸ In 2008, Bickelhaupt group proposed the “ball in a box” model to rationalize why the [Cl-CH₃-Cl]⁻ TBPC structure (Scheme 1-IV) is a TS, while the [Cl-SiH₃-Cl]⁻ analog (Scheme 1-V) is a minimum.¹⁹ After that, in 2009 they further suggested to use more rigid planar CR₃• as the equatorial moiety to stabilize

^{a)}Authors to whom correspondence should be addressed. Electronic addresses: wyb@sxu.edu.cn and zwxwang@ucas.ac.cn



SCHEME 1. Structures of some species mentioned in the text.

the TBPC arrangement, and found that the σ -donating and π -accepting CN group significantly enhance the planarity of $C(CN)_3$ unit. Among their reported species, the anionic D_{3h} $[X-C(CN)_3-X]^-$ ($X = F, Cl,$ and Br) are not minima, the D_{3h} $[I-C(CN)_3-I]^-$ may be a minimum, depending on the basis set used, but the D_{3h} $[At-C(CN)_3-At]^-$ (Scheme 1-VI) is a minimum regardless of used basis sets.²⁰ To our knowledge, this is the first example of anionic TBPC species, but whether this species is a global minimum was not investigated. Herein, we report a strategy to obtain a class of TBPC structures, $[A-CE_3-A]^-$ ($E = Al$ and $Ga, A = Si, Ge, Sn,$ and Pb), as well as their electronic structures. These hexatomic clusters are all energy minima. Of particular interest, $[Ge-CAI_3-Ge]^-$ and $[Sn-CGa_3-Sn]^-$ are global minima, which indicates that these two species could be formed easily by the laser vaporization in the gas phase and characterized by experiments such as the size-selected negative ion photoelectron spectroscopy.

II. COMPUTATIONAL DETAILS

For the heavy elements, Ga, Ge, Sn, and Pb, the relativistic effect was considered by using the correlation-consistent-like basis set aug-cc-pVDZ-PP^{21,22} and aug-cc-pVTZ-PP^{21,22} with accurate small-core relativistic pseudopotentials. The potential energy surfaces (PESs) were probed using stochastic search algorithm.^{23,24} Random structures were initially generated by GXYZ program^{25,26} and then subjected to geometry optimizations at the B3LYP/BSI level, where BSI denotes 6-31+G(d) for C, Al, and Si, and aug-cc-pVDZ-PP for Ga, Ge, Sn, and Pb. To ascertain the convergence of the PES explorations, we run three sets of searches on the singlet PESs and two sets on the triplet PESs for each of total eight A-CE₃-A ($E = Al$ and Ga and $A = Ga, Ge, Sn,$ and Pb) stoichiometries. The 20 lowest isomers of each stoichiometry were reoptimized and characterized to be energy minima at the B3LYP/BSII level (BSII denotes aug-cc-pVTZ for C, Al, and Si and aug-cc-pVTZ-PP for Ga, Ge, Sn, and Pb). The MP2/BSII calculations were also performed for the five lowest isomers to verify the minimum characteristics given by the B3LYP/BSII vibrational frequency calculations. Finally, the geometries of these five isomers of each stoichiometry were refined at the CCSD(T)/BSII level. The T1 diagnostic values of the converged CCSD(T)/BSII wavefunctions for **1a-8a** (see Figure 1) range from 0.020 to 0.028 and those for other isomers range from 0.023 to 0.042, thus the multi-reference

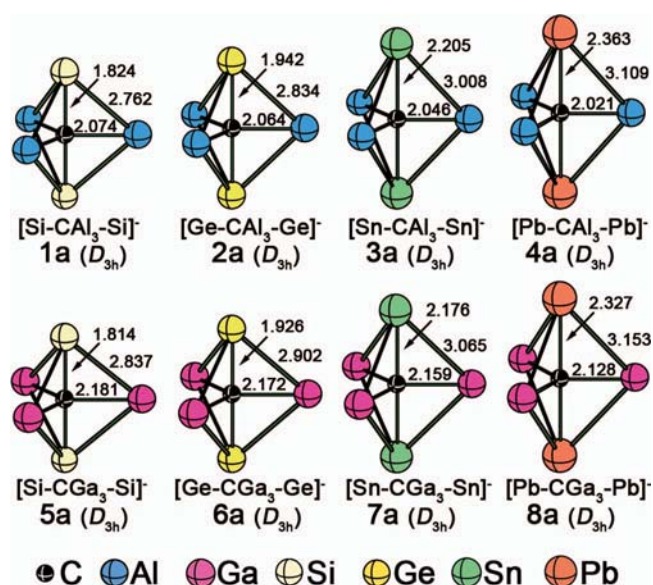


FIG. 1. CCSD(T)/BSII optimized structures of eight hexatomic mono-anionic TBPC species. All the key bond lengths are given in Å.

characters are not important. The structures and relative energies at this level were discussed in the text. The natural bond orbital (NBO)²⁷ analysis calculations were carried out at the B3LYP/BSII level to gain insight into the bonding nature. The detailed adaptive natural density partitioning (AdNDP)²⁸⁻³⁰ analyses at the B3LYP/6-31G (LANL2DZ for Sn and Pb) level were performed to interpret the bonding patterns. The vertical detachment energies (VDE) were calculated by the outer-valence Green's function (OVGF) procedure at the OVGF/BSII level. The random coordinates were generated from GXYZ program, the CCSD(T) optimizations were performed by using MOLPRO 2008.1 package,³¹ and other calculations were carried out by using GAUSSIAN 03 and 09 packages.^{32,33}

III. RESULTS AND DISCUSSION

A. The strategy

To achieve the non-classical phC structures, one strategy among others is to use electropositive atoms/ligands (e.g., Be, B, and Al or groups containing them) to soften the rigidity of tetrahedral sp^3 carbon bonding, because the electron donation of the electropositive ligands can weaken the directionality of sp^3 hybridization.³⁴⁻⁴⁴ Similarly, we hypothesized that such an electronic effect can be applied to achieve the non-classical TBPC species. In fact, this can be applied to understand the previously reported TBPC structures. For example, Frenking group found computationally that, when replacing the SiH_3 groups in **III** with other electropositive groups (XH_3 , $X = Ge-Pb$, or XH_2 , $X = B-In$), all analogs of **III** are the TBPC minima.¹⁵ As for the series of $[X-C(CN)_3-X]^-$ ($X = F, Cl, Br, I, At$) mono-anions, when X goes from F to At, the covalent bonding character of C-X bond decreases, thus the TBPC structure becomes more and more feasible.²⁰

TABLE I. The lowest vibrational frequencies (ν_{\min}), the HOMO-LUMO energy gaps (Gap), and the NBO analysis results, including the natural charges of C, the equatorial E atoms, and the apical A atoms (Q_C , Q_E , and Q_A), the total Wiberg bond indices of these atoms (WBI_C, WBI_E, and WBI_A), and the Wiberg bond orders including C–E, C–A, E–A, and A–A (WBI_{C–E}, WBI_{C–A}, WBI_{E–A}, and WBI_{A–A}) of **1a–8a** at B3LYP/BSII level.

	ν_{\min}	Gap	Q_C	Q_E	Q_A	WBI _C	WBI _E	WBI _A	WBI _{C–E}	WBI _{C–A}	WBI _{E–A}	WBI _{A–A}
[Si-CAl ₃ -Si] [−] (1a)	104	2.85	−2.64	0.52	0.05	2.55	1.15	2.84	0.25	0.89	0.38	0.79
[Ge-CAl ₃ -Ge] [−] (2a)	96	2.78	−2.60	0.50	0.05	2.53	1.17	2.79	0.28	0.84	0.37	0.82
[Sn-CAl ₃ -Sn] [−] (3a)	76	2.50	−2.78	0.46	0.20	2.34	1.34	2.66	0.36	0.63	0.41	0.79
[Pb-CAl ₃ -Pb] [−] (4a)	59	2.29	−2.77	0.46	0.19	2.31	1.38	2.60	0.40	0.56	0.41	0.81
[Si-CGa ₃ -Si] [−] (5a)	66	2.54	−2.39	0.41	0.08	2.74	1.18	2.80	0.28	0.95	0.38	0.72
[Ge-CGa ₃ -Ge] [−] (6a)	63	2.51	−2.35	0.40	0.07	2.77	1.20	2.75	0.31	0.92	0.36	0.76
[Sn-CGa ₃ -Sn] [−] (7a)	57	2.36	−2.50	0.35	0.23	2.59	1.32	2.62	0.38	0.72	0.37	0.79
[Pb-CGa ₃ -Pb] [−] (8a)	48	2.19	−2.47	0.34	0.23	2.60	1.35	2.57	0.43	0.66	0.36	0.84

B. Design and characterization of TBPC species

Al atom has been used to realize various pH_C species.^{24,34–36,39–50} Because Al is metallic with appreciable non-metallic character, the C–Al bond is mainly ionic, which helps to soften the rigidity of tetrahedral carbon, and on the other hand, it bears the weak covalent bonding character, which helps to maintain the hypercoordination skeleton. Thus to make a start, we tried to take CAL₃ as the middle fragment of the TBPC structure and searched for proper axial atoms by scanning the first three rows of the p-block elements. Delightfully, among 15 candidates, the D_{3h} [A-CAl₃-A][−] (A = Si (**1a**) and Ge (**2a**)) were found to be the energy minima with stable wavefunctions at the B3LYP/BSII level. On the basis of **1a** and **2a**, more TBPC species were found by using Al or Ga as the equatorial atoms (E) and Si, Ge, Sn, and Pb as the axial atoms (A). The resulted eight D_{3h} structures, including **1a** and **2a**, are all energy minima at both the B3LYP/BSII and MP2/BSII levels. Their CCSD(T)/BSII optimized geometries are shown in Fig. 1. The equatorial C–Al distances ($R_{C–Al}$) in **1a–4a** range from 2.021 to 2.074 Å and C–Ga distances ($R_{C–Ga}$) in **5a–8a** from 2.128 to 2.181 Å. The distances of axial C–Si in **1a/5a**, C–Ge in **2a/6a**, C–Sn in **3a/7a**, and C–Pb in **4a/8a** are 1.824/1.814, 1.942/1.926, 2.205/2.176, and 2.363/2.327 Å, respectively. All these interatomic distances are within the typical bond lengths.

The NBO results, listed in Table I, rationalize the stabilization of these TBPC species. At first, despite the hypercoordination, the bonding of the central carbon atoms in **1a–8a** obeys the octet rule. The total Wiberg bond indices (WBI_C) on the central carbon atoms (denoted as TBP-C hereafter) range from 2.31 to 2.77, which contribute 4.62 to 5.54 |e| to the electron counts on TBPCs. After inclusion of the negative charges (Q_C) on TBPCs, the total electron counts on TBP-Cs are less than 8.0, ranging from 7.39 to 7.89 |e|. Second, the total WBI_C, ranging from 2.31 to 2.77, are significantly smaller than 4. The reduced covalent bonding character, as mentioned above, benefits the stabilization of hypercoordination bonding. Third, the C–E bonds with WBI_{C–E} values (0.25–0.43) and the C–A bonds with WBI_{C–A} values (0.56–0.95) indicate the substantial covalent bonding character of these bonds, which helps to hold the TBPC skeleton. Finally, the stabilization of the TBPC benefits from the cage enforcement; there are substantial covalent bonding interactions among the equatorial E, axial A atoms, and central C atom, as evidenced by

the WBI_{E–A}, WBI_{C–E}, and WBI_{C–A} values in Table I. In terms of the “ball-in-box” model, the formation of efficient E–A, C–A, and A–C–A covalent bonding diminishes the space of the E₃A₂ “box,” so the central carbon atom can be lifted from the bottom to the center of the box.

The degenerate LUMOs and occupied valence molecular orbitals (MO) of **1a** are depicted in Fig. 2 and the similar MOs of **2a–8a** are given in the supplementary material.⁵¹ As shown in Fig. 2, in the degenerate HOMO, the p_x or p_y atomic orbitals of Si bridge the p_z atomic orbitals of Al atoms, forming a peripheral bonding around TBPC. These two bonding orbitals contribute to WBI_{E–A}. Similar peripheral bonding orbitals exist in ptC species/molecules such as CAL₄[−],³⁹ C₂Al₄,²⁴ boraplanes,⁵² and neutral species with C(C)₄ unit⁵³ and were considered to be the key factor for the stabilization of the ptC arrangement. The axial parts of HOMO–3 and degenerated HOMO–1 clearly show the linear Si–C–Si 3-center bonding characters, which are majorly responsible for the large WBI_{Si–Si} value (0.79) but with the significantly long interatomic Si–Si distance (3.616 Å at the B3LYP/BSII level). HOMO–2 and HOMO–6 correspond to the axial C–Si bonding. The degenerate HOMO–5 contributes to C–Al bonding.

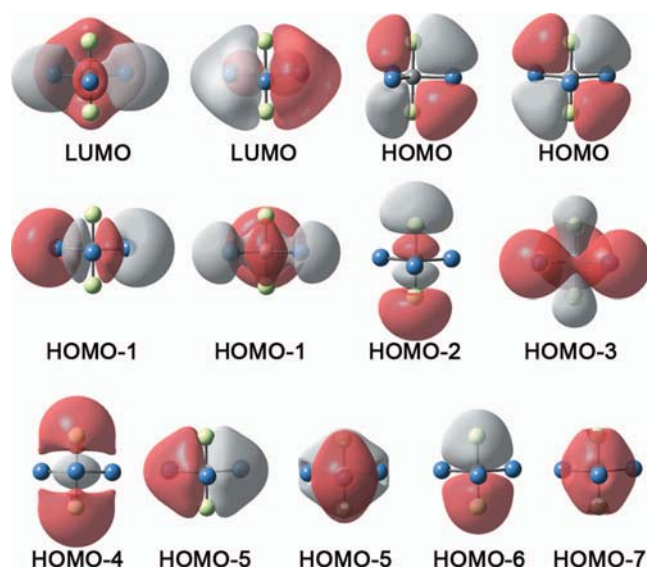


FIG. 2. Degenerate LUMOs and occupied valence molecular orbitals of [Si-CAl₃-Si][−].

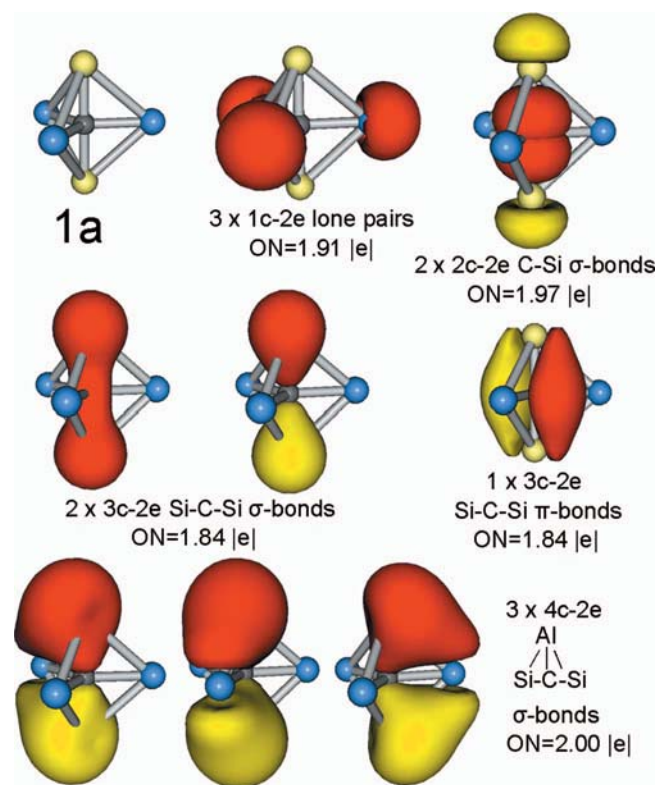


FIG. 3. AdNDP bonding pattern obtained for $[\text{Si-CAl}_3\text{-Si}]^-$ with occupation numbers indicated.

The detailed AdNDP analyses have revealed the bonding patterns more clearly. As shown in Fig. 3, there are five types of the occupied electrons in **1a**, namely, three one-center-two-electron (1c-2e) lone pairs with occupation number (ON) of 1.91 |e|, two two-center-two-electron (2c-2e) C-Si σ -bonds (ON = 1.97 |e|), two three-center-two-electron (3c-2e) Si-C-Si σ -bonds (ON = 1.84 |e|), one 3c-2e Si-C-Si π -bond (ON = 1.84 |e|), and three four-center-two-electron (4c-2e) Si-C-Si-Al σ -bonds (ON = 2.00 |e|). The multiple-center bonding contributes to the stabilization of TBPC structure. For example, both 3c-2e σ -bonds and π -bond contribute to the rigidity of Si-C-Si axis and the 4c-2e σ -bonds to the peripheral cage refinement. The AdNDP results for other TBPC species are given in the supplementary material.⁵¹ For TBPC species with axial Si or Ge atoms, corresponding species **2a**, **5a**, and **6a** have very similar AdNDP partitioning pattern for the occupied electrons. For those with axial Sn atoms (**3a** and **7a**), the two 3c-2e σ -bonds in **1a** become lone pairs, but the 3c-2e π -bond remains unchanged. For those with axial Pb atoms (**4a** and **8a**), the 3c-2e π -bond in **3a** or **7a** becomes a 6c-2e σ -bond, which distributes more on Pb-C-Pb axis. Nevertheless, both the 3c-2e σ -bond in TBPC species with axial Si, Ge, or Sn atoms and the 6c-2e σ -bond in those with axial Pb atoms play an important role in keeping the rigidity of A-C-A axis.

C. Thermodynamic and kinetic stabilities

The species **1a**–**8a** are the simplest anions with TBPC arrangement, which benefits their generation in the experiments. An effective experimental approach to capture such

species could be the photoelectron spectroscopy. Previously, the smallest ptC species such as Al_4^- , NaAl_4^- , Al_3Si^- , and Al_3Ge^- have been identified by PES.^{39–42} In a PES experiment, a targeted species is generated in the gas phase thermodynamically, and thus the abundances of isomers are controlled by their relative free energies on the basis of the Boltzmann distribution. To capture a targeted species in a PES experiment, it is highly desired that the species is a low-lying isomer among many possible isomers. Indeed, the PES-observed ptC species were all computationally verified to be global minima. To assess the experimental viability of our predicted TBPC species, we further explored the potential energy surfaces of CE_3A_2^- ($E = \text{Al/Ga}$ and $A = \text{Si-Pb}$) using stochastic search algorithm. Fig. 4 shows the CCSD(T) geometric and energetic results of the four lowest isomers of **1a**, **2a**, **6a**, and **7a**, the results for **3a**–**5a** and **8a** are given in the supplementary material.^{49,51} Remarkably, **2a** and **7a** were found to be the global minima at the CCSD(T)/BSII level, and the second lowest isomers (**2b** and **7b**) are 0.75 and 0.77 kcal/mol higher than **2a** and **7a**, respectively. **1a** is the second lowest isomer, but it is only 0.01 kcal/mol higher than the global minimum **1b**. **6a** is the second lowest isomer that is 0.82 kcal/mol higher than the global minimum **6b**. Other isomers, **1c**, **2c**, **6c**, and **7c**, are substantially higher than the TBPC structures by 4.71, 1.09, 3.35, and 2.03 kcal/mol. However, **3a**–**5a** and **8a** are relatively high energy isomers; they are 2.26, 8.00, 2.60, and 3.28 kcal/mol higher than their corresponding global minima (**3b**, **4b**, **5b**, and **8b**), respectively. We have omitted these species from further discussion in the following.

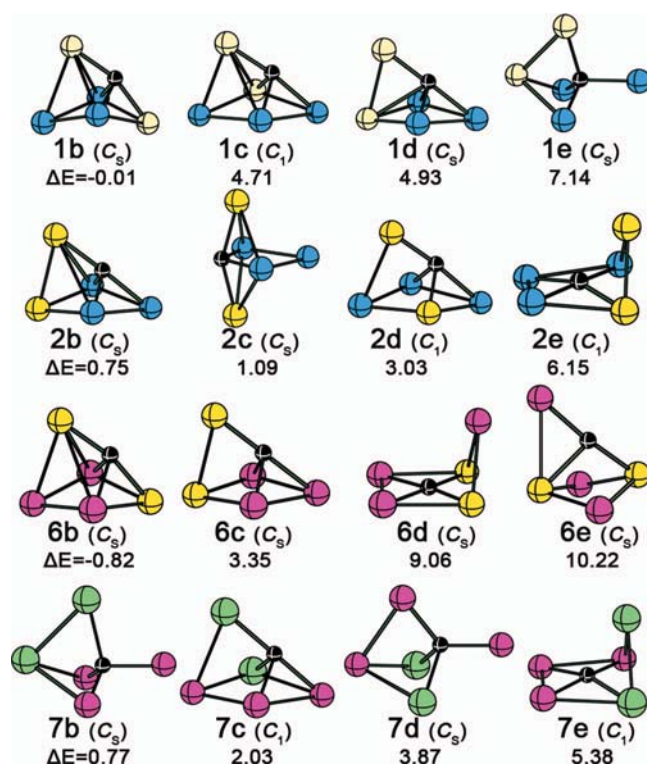


FIG. 4. The CCSD(T)/BSII optimized structures, the point groups (in parentheses) and the relative energies (in kcal/mol) of other four lowest isomers of **1a**, **2a**, **6a**, and **7a**. The energies of TBPC isomers were referred as zero.

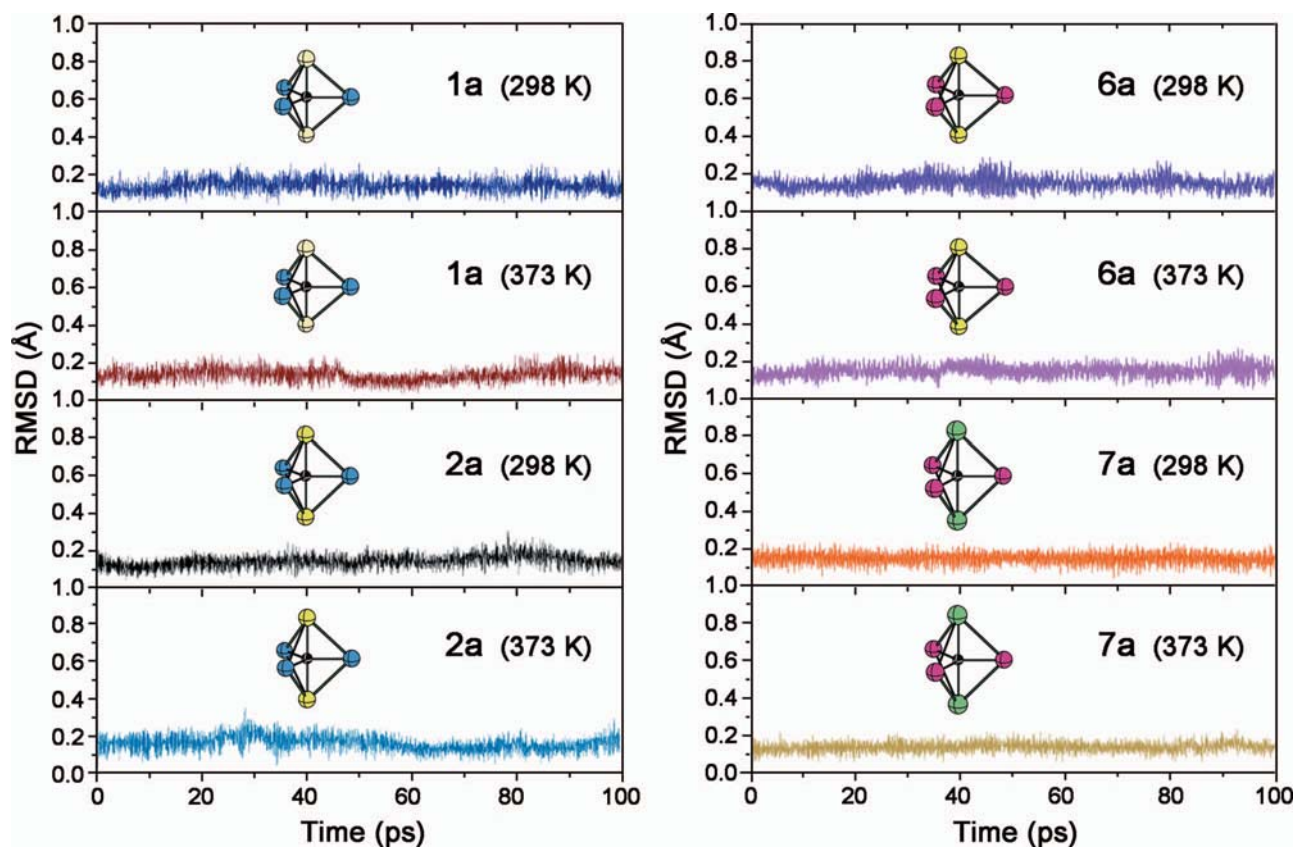


FIG. 5. RMSDs vs. simulation time for **1a**, **2a**, **6a**, and **7a** at both 298 and 373 K.

The kinetic stabilities of **1a**, **2a**, **6a**, and **7a** are further evaluated by the Born-Oppenheimer molecular dynamics (BOMD) simulation and isomerization reaction studies at density functional theory level. Because no isomers composing of two or more fragments were found, the most possible decay pathway for the four thermodynamically favorable species should be isomerization rather than dissociation. Taking $\text{CAI}_3\text{Si}_2^-$ as an example, the isomer **1b** is very similar in structure to TBPC species **1a** and the isomerization of **1a** to **1b** only needs to squeeze the carbon in **1a** out of the molecular center. The energy barrier for the process was predicted to be 9.02 kcal/mol at B3LYP/aug-cc-pVTZ level. Similar isomers were found for **2a**, **6a**, and **7a**. At B3LYP/aug-cc-pVTZ (aug-cc-pVTZ-PP for Ga, Ge, and Sn) level, the energy barriers for the isomerizations were calculated to be 9.98, 8.87, and 10.04 kcal/mol, respectively.

BOMD simulations at B3LYP/6-31G(d) (cc-pVDZ-PP for Ga, Ge, and Sn) level also suggested **1a**, **2a**, **6a**, and **7a** possess the very high kinetic stability. As shown in Fig. 5, the root-mean-square deviation (RMSD) curves in all these simulations have no significant increase, suggesting that the TBPC structures can be well-maintained at both 298 and 373 K during the simulation. The fluctuation of RMSD values is very small: the minimum values range from 0.04 to 0.07 Å, the maximum values range from 0.23 to 0.35 Å, and the average values range from 0.14 to 0.16 Å, respectively. Throughout the dynamic simulation, we could not see any indication of destruction of the TBPC structures.

On the basis of the study of the thermodynamic and kinetic stabilities of these species, we predict that the mono-

anionic global minima (**2a** and **7a**) are very promising for experimental realization and **1a** and **6a**, which are close to global minima, could also have chance to be observed using the laser-ablation/vaporization or arc discharge techniques followed by the characterization in the negative ion photoelectron spectroscopy.

D. Vertical detachment energies

To aid the experimental observation, we computed the vertical detachment energies of these species at the OVGf/BSII level. Because **1b**, **2b**, **6b**, and **7b** are energetically competitive, we also calculated their VDEs to see whether the PES peaks can be resolved. The VDEs of **1a**, **2a**, **6a**, and **7a** were turned out to be 3.00, 2.83, 2.41, and 2.32 eV, respectively, which are all larger than those of their close isomers, being 2.49 (**1b**), 2.66 (**2b**), 2.27 (**6b**), and 2.26 (**7b**) eV, respectively. Since the HOMOs of these TBPC species are all degenerate, the PES peaks should be very high and could be regarded as the spectroscopic fingerprints of these species.

IV. CONCLUSIONS

The electropositive ligands have stabilization effect on pHc arrangement, which stems from the electron donation of such ligands that soften the rigid tetrahedral arrangement of sp^3 carbon bonding via weakening the directionality of sp^3 hybridization. Using a similar strategy, we designed a new class of the hexatomic mono-anionic species with non-classical TBPC bonding, $D_{3h}[\text{A-CE}_3\text{-A}]^-$ (E = Al and

Ga, A = Si, Ge, Sn, and Pb). The explorations of their potential energy surfaces at the B3LYP level and the elaborated examinations at the MP2 and CCSD level show that the eight species (**1a–8a**) are all minima, among which $[\text{Ge-CAl}_3\text{-Ge}]^-$ (**2a**) and $[\text{Sn-CGa}_3\text{-Sn}]^-$ (**7a**) are the global minima and $[\text{Si-CAl}_3\text{-Si}]^-$ (**1a**) and $[\text{Ge-CGa}_3\text{-Ge}]^-$ (**6a**) are the energetically competitive lowest local minima. The BOMD simulations and isomerization barriers indicate that the four species are kinetically stable. The electronic structure analyses reveal that the substantial ionic C–E bonding, the peripheral E–A covalent bonding, and the linear axial A–C–A multi-center-two electrons (mc-2e) bonding play roles in stabilizing these TBPC structures. The structural simplicity and the high thermodynamic stabilities of these species (**1a**, **2a**, **6a**, and **7a**) suggest that they may be generated and captured in the gas phase. Furthermore, as mono-anionic species, their first vertical detachment energies are differentiable from those of their nearest isomers, which would facilitate their characterization via experiments such as the negative ion photoelectron spectroscopy.

ACKNOWLEDGMENTS

This paper is dedicated to Professor Pin Yang on the occasion of his 80th birthday. The present work is supported financially by the National Natural Science Foundation of China (NSFC) (Grant Nos. 21003086, 21273140, 21173263, and 21373216), Natural Science Foundation of Shanxi Province (SXNSF) (Grant No. 2009021016), and the Foundation of State Key Laboratory of Theoretical and Computational Chemistry (Grant No. K1104). Y.-B.W. thanks Professor Yue-Kui Wang for constructive discussion.

- ¹R. Hoffmann, R. W. Alder, and C. F. Wilcox, Jr., *J. Am. Chem. Soc.* **92**, 4992 (1970).
- ²J. B. Collins, J. D. Dill, E. D. Jemmis, Y. Apeloig, P. v. R. Schleyer, R. Seeger, and J. A. Pople, *J. Am. Chem. Soc.* **98**, 5419 (1976).
- ³K. Sorger and P. v. R. Schleyer, *J. Mol. Struct.: THEOCHEM*, **338**, 317 (1995).
- ⁴D. Rottger and G. Erker, *Angew. Chem., Int. Ed. Engl.* **36**, 812 (1997).
- ⁵L. Radom and D. R. Rasmussen, *Pure Appl. Chem.* **70**, 1977 (1998).
- ⁶W. Siebert and A. Gunale, *Chem. Soc. Rev.* **28**, 367 (1999).
- ⁷R. Keese, *Chem. Rev.* **106**, 4787 (2006).
- ⁸G. Merino, M. A. Mendez-Rojas, A. Vela, and T. Heine, *J. Comput. Chem.* **28**, 362 (2007).
- ⁹J. I. Musher, *Angew. Chem., Int. Ed.* **8**, 54 (1969).
- ¹⁰T. R. Forbus and J. C. Martin, *J. Am. Chem. Soc.* **101**, 5057 (1979).
- ¹¹J. C. Martin, *Science* **221**, 509 (1983).
- ¹²E. D. Jemmis, J. Chandrasekhar, and P. v. R. Schleyer, *J. Am. Chem. Soc.* **101**, 527 (1979).
- ¹³E. D. Jemmis, J. Chandrasekhar, E.-U. Wurthwein, and P. v. R. Schleyer, *J. Am. Chem. Soc.* **104**, 4275 (1982).
- ¹⁴J. Z. Davalos, R. Herrero, J. M. Abboud, O. Mo, and M. Yanez, *Angew. Chem., Int. Ed.* **46**, 381 (2007).
- ¹⁵I. Fernandez, E. Uggerud, and G. Frenking, *Chem.-Eur. J.* **13**, 8620 (2007).
- ¹⁶J. W. Chinn, Jr. and R. J. Lagow, *J. Am. Chem. Soc.* **106**, 3694 (1984).
- ¹⁷K. Y. Akiba, Y. Moriyama, M. Mizozoe, H. Inohara, T. Nishii, Y. Yamamoto, M. Minoura, D. Hashizume, F. Iwasaki, N. Takagi, K. Ishimura, and S. Nagase, *J. Am. Chem. Soc.* **127**, 5893 (2005).
- ¹⁸M. Yamashita, Y. Yamamoto, K. Y. Akiba, D. Hashizume, F. Iwasaki, N. Takagi, and S. Nagase, *J. Am. Chem. Soc.* **127**, 4354 (2005).
- ¹⁹S. C. A. H. Pierrefixe, C. F. Guerra, and F. M. Bickelhaupt, *Chem.-Eur. J.* **14**, 819 (2008).
- ²⁰S. C. A. H. Pierrefixe, S. J. M. van Stralen, J. N. P. van Stralen, C. F. Guerra, and F. M. Bickelhaupt, *Angew. Chem., Int. Ed.* **48**, 6469 (2009).
- ²¹K. A. Peterson, *J. Chem. Phys.* **119**, 11099 (2003).
- ²²K. A. Peterson, D. Figgen, E. Goll, H. Stoll, and M. Dolg, *J. Chem. Phys.* **119**, 11113 (2003).
- ²³M. Saunders, *J. Comput. Chem.* **25**, 621 (2004).
- ²⁴P. P. Bera, K. W. Sattelmeyer, M. Saunders, H. F. Schaefer, and P. v. R. Schleyer, *J. Phys. Chem. A* **110**, 4287 (2006).
- ²⁵H. G. Lu and Y. B. Wu, *GXYZ, A Random Cartesian Coordinates Generating Program* (Shanxi University, Taiyuan, 2008).
- ²⁶Y. B. Wu, H. G. Lu, S. D. Li, and Z. X. Wang, *J. Phys. Chem. A* **113**, 3395 (2009).
- ²⁷A. E. Reed, L. A. Curtiss, and F. Weinhold, *Chem. Rev.* **88**, 899 (1988).
- ²⁸D. Y. Zubarev and A. I. Boldyrev, *Phys. Chem. Chem. Phys.* **10**, 5207 (2008).
- ²⁹D. Y. Zubarev and A. I. Boldyrev, *J. Org. Chem.* **73**, 9251 (2008).
- ³⁰D. Y. Zubarev and A. I. Boldyrev, *J. Phys. Chem. A* **113**, 866 (2009).
- ³¹H. J. Werner, P. J. Knowles, R. Lindh, F. R. Manby, M. Schütz *et al.*, MOLPRO version 2008.1, a package of *ab initio* programs, 2008, see <http://www.molpro.net>.
- ³²M. J. Frisch, G. W. Trucks, H. B. Schlegel *et al.*, GAUSSIAN 03, Revision C.02, Gaussian, Inc., Wallingford, CT, 2004.
- ³³M. J. Frisch, G. W. Trucks, H. B. Schlegel *et al.*, GAUSSIAN 09, Revision D.01, Gaussian Inc., Wallingford, CT, 2009.
- ³⁴Z. X. Wang, C. G. Zhang, Z. F. Chen, and P. v. R. Schleyer, *Inorg. Chem.* **47**, 1332 (2008).
- ³⁵Y. B. Wu, J. L. Jiang, H. G. Lu, Z. X. Wang, N. Perez-Peralta, R. Islas, M. Contreras, G. Merino, J. I. C. Wu, and P. v. R. Schleyer, *Chem.-Eur. J.* **17**, 714 (2011).
- ³⁶Y. B. Wu, Y. Duan, H. G. Lu, and S. D. Li, *J. Phys. Chem. A* **116**, 3290 (2012).
- ³⁷Y. B. Wu, J. L. Jiang, R. W. Zhang, and Z. X. Wang, *Chem.-Eur. J.* **16**, 1271 (2010).
- ³⁸Y.-B. Wu, Y. Duan, G. Lu, H.-G. Lu, P. Yang, P. v. R. Schleyer, G. Merino, R. Islas, and Z.-X. Wang, *Phys. Chem. Chem. Phys.* **14**, 14760 (2012).
- ³⁹X. Li, L. S. Wang, A. I. Boldyrev, and J. Simons, *J. Am. Chem. Soc.* **121**, 6033 (1999).
- ⁴⁰L. S. Wang, A. I. Boldyrev, X. Li, and J. Simons, *J. Am. Chem. Soc.* **122**, 7681 (2000).
- ⁴¹X. Li, H. F. Zhang, L. S. Wang, G. D. Geske, and A. I. Boldyrev, *Angew. Chem., Int. Ed.* **39**, 3630 (2000).
- ⁴²X. Li, H. J. Zhai, and L. S. Wang, *Chem. Phys. Lett.* **357**, 415 (2002).
- ⁴³Z. X. Wang, T. K. Manojkumar, C. Wannere, and P. V. R. Schleyer, *Org. Lett.* **3**, 1249–1252 (2001).
- ⁴⁴Z.-H. Cui, M. Contreras, Y.-H. Ding, and G. Merino, *J. Am. Chem. Soc.* **133**, 13228–13231 (2011).
- ⁴⁵H. B. Xie and Y. H. Ding, *J. Chem. Phys.* **126**, 184302 (2007).
- ⁴⁶Y. Pei, W. An, K. Ito, P. v. R. Schleyer, and X. C. Zeng, *J. Am. Chem. Soc.* **130**, 10394 (2008).
- ⁴⁷Z. H. Cui, C. B. Shao, S. M. Gao, and Y. H. Ding, *Phys. Chem. Chem. Phys.* **12**, 13637 (2010).
- ⁴⁸F. Dong, S. Heinbuch, Y. Xie, J. J. Rocca, and E. R. Bernstein, *Phys. Chem. Chem. Phys.* **12**, 2569 (2010).
- ⁴⁹J. O. C. Jimenez-Halla, Y. B. Wu, Z. X. Wang, R. Islas, T. Heine, and G. Merino, *Chem. Commun.* **46**, 8776 (2010).
- ⁵⁰A. C. Castro, G. Martinez-Guajardo, T. Johnson, J. M. Ugalde, Y.-B. Wu, J. M. Mercero, T. Heine, K. J. Donald, and G. Merino, *Phys. Chem. Chem. Phys.* **14**, 14764 (2012).
- ⁵¹See supplementary material at <http://dx.doi.org/10.1063/1.4867364> for the MO plots and the AdNDP analysis results of **2a–8a** and the CCSD(T)/BSII optimized geometries (in Cartesian coordinates) and absolute energies (in Hartree) of five lowest isomers of $[\text{A-CE}_3\text{-A}]^-$ (E = Al and Ga, A = Si, Ge, Sn, and Pb).
- ⁵²Z. X. Wang and P. v. R. Schleyer, *J. Am. Chem. Soc.* **123**, 994 (2001).
- ⁵³Z. X. Wang and P. v. R. Schleyer, *J. Am. Chem. Soc.* **124**, 11979 (2002).